

**EFFECT OF HEAT TREATMENT AND LASER
SURFACE TREATMENT ON THE CORROSION
BEHAVIOR OF STAINLESS STEELS**

by

Chan Weng Kin



M.Sc. in Electromechanical Engineering

2010/2011



**Faculty of Science and Technology
University of Macau**

EFFECT OF HEAT TREATMENT AND LASER SURFACE
TREATMENT ON THE CORROSION BEHAVIOR OF
STAINLESS STEELS

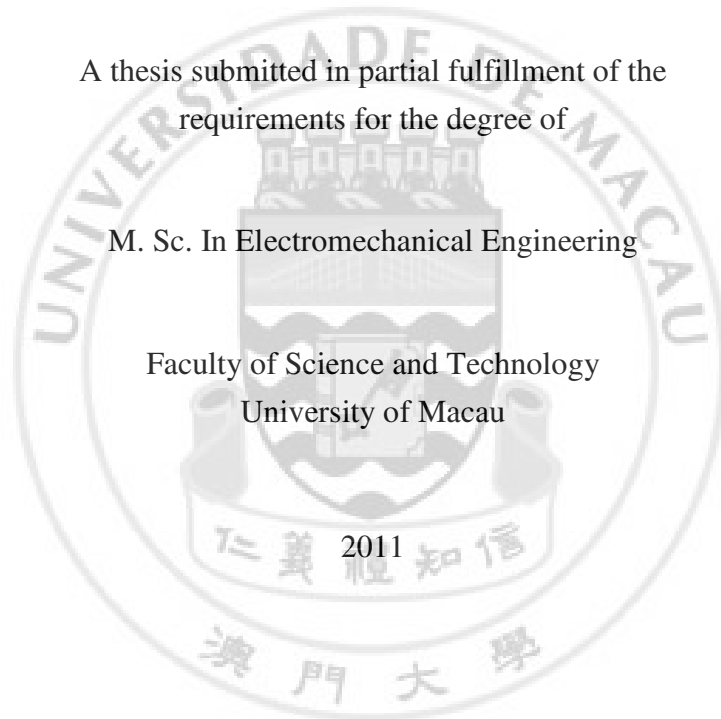
by

Chan Weng Kin

A thesis submitted in partial fulfillment of the
requirements for the degree of

M. Sc. In Electromechanical Engineering

Faculty of Science and Technology
University of Macau



Approved by _____

Supervisor

Co-supervisor

Date _____

In presenting this thesis in partial fulfillment of the requirements for a Master's degree at the University of Macau, I agree that the Library and the Faculty of Science and Technology shall make its copies freely available for inspection. However, reproduction of this thesis for any purposes or by any means shall not be allowed without my written permission. Authorization is sought by contacting the author at

Address: PATIO PILOTO 19-23, ED. FU VA GARDEN, 4 ANDAR G,
MACAU

Telephone: (853) 66983661

Fax:

E-mail: ma96540@umac.mo, ericchan0627@hotmail.com



Signature _____

Date _____

University of Macau

Abstract

EFFECT OF HEAT TREATMENT AND LASER SURFACE
TREATMENT ON THE CORROSION BEHAVIOR OF
STAINLESS STEELS

by Chan Weng Kin

Thesis Supervisor:

Prof. Kwok Chi Tat

Thesis Co-supervisor:

Dr. Lo Kin Ho

M. Sc. In Electromechanical Engineering

In the present study, the effect of heat and laser treatment on intergranular corrosion (IGC) and pitting corrosion behavior of various austenitic stainless steels ASSs (UNS S30400, S31603, S32100, S34700, FeCrMn), duplex stainless steels DSSs (S31803 and S32950) and super duplex stainless steel SDSS (S32760) were investigated. Double loop electrochemical potentiokinetic reactivation (DL-EPR) test was performed by using a potentiostat on aged ASSs in 0.5 M H₂SO₄ + 0.01 M KSCN solution at 25 °C whereas for aged DSSs and SDSS, a more aggressive solution (2 M H₂SO₄, 0.01 M KSCN and 0.5 M NaCl at 25 °C) was used. SEM examination revealed that intergranular attack occurs at the Cr-depleted grain boundaries for the aged ASSs while attack takes place at the phase boundaries of the intermetallic σ phase and metallic phase (γ , δ , γ_2) for the aged DSSs. Cyclic potentiodynamic polarization was also carried out for investigating the pitting corrosion behavior of various aged stainless steels in 3.5 wt% NaCl solution at 25°C. For FeCrMn, increase in the aging time significantly deteriorates the pitting resistance and the specimens

even do not passive when the aging time is longer than 50 h. For aged S31803 and S32950, the pitting resistance is also deteriorated as evidenced by the decrease in pitting potential. Similar results are obtained for aged S32760, but higher repassivation ability was observed mainly due to the present of more passivable alloying elements.

Laser surface melting (LSM) was done on various stainless steels by a 2.5-kW CW Nd:YAG laser and a 2.3-kW diode laser. Different laser processing parameters were applied to melt the surface of FeCrMn and S32950 for optimizing the LSM conditions for corrosion resistance. The pitting resistance of the aged S32950 after LSM with a higher scanning speed and lower power of the laser is higher than that of the ones fabricated with a lower processing speed or higher power. In addition, the aged ASSs were essentially austenitic with some δ (except FeCrMn) but the chromium carbides were completely removed after LSM. For the aged DSS and SDSS after LSM, δ became the major phase and the δ/γ phase balance was disturbed but the σ and γ_2 phases were eliminated. After LSM, the IGC resistance of the aged ASSs was found to be considerably improved as reflected by the reduction in degree of sensitization (DOS). This could be attributed to a more homogenous microstructure and the redissolution of chromium carbides. The IGC resistance of aged DSSs and SDSS was also significantly enhanced as indicated by the decrease in DOS. This could be attributed to a more homogenous microstructure and to the redissolution of σ and γ_2 phases. Furthermore, the effects of re-aging after LSM were also investigated on FeCrMn and S32950. Both of them showed higher pitting resistance as compared with that of the aged specimens.

TABLE OF CONTENTS

LIST OF FIGURES.....	vi
LIST OF TABLES.....	xiii
LIST OF ABBREVIATIONS.....	xv
LIST OF PUBLICATIONS.....	xvi
ACKNOWLEDGEMENTS.....	xviii
CHAPTER 1: Introduction	
1.1 Research Background.....	1
1.2 Objectives.....	3
CHAPTER 2: Literature Review	
2.1 Role of alloying elements in stainless steels.....	4
2.1.1 Ferritic stainless steels.....	6
2.1.2 Austenitic stainless steels.....	6
2.1.2.1 Common grade ASSs.....	7
2.1.2.2 Stabilized grade ASSs.....	8
2.1.2.3 Ni-free grade ASSs.....	9
2.1.3 Duplex stainless steels.....	10
2.1.3.1 Lean grade DSSs.....	11
2.1.3.2 Super DSSs and hyper DSSs.....	11
2.2 Effect of thermal aging on stainless steels.....	12
2.2.1 Sensitization of austenitic stainless steels.....	12
2.2.2 Sensitization of duplex stainless steels.....	14

2.3 Laser surface treatment.....	17
2.3.1 Laser surface melting.....	18
2.3.2 Advantages of LSM.....	19
2.3.3 Heat transfer model of LSM.....	20
2.3.4 Applications of LSM.....	23
2.4 Corrosion of stainless steels.....	24
2.4.1 General corrosion.....	25
2.4.2 Pitting corrosion.....	27
2.4.2.1 Pitting corrosion test.....	27
2.4.3 Intergranular corrosion.....	30
2.4.3.1 Intergranular corrosion test.....	31
2.5 Review of current research of LSM of stainless steels.....	33
2.5.1 IGC behaviors of LSM of stainless steels.....	33
2.5.1.1 Effect of LSM, LSA and LC.....	34
2.5.1.2 LSM of weldments.....	35
2.5.1.3 Effect of cooling rate (δ -ferrite content).....	35
2.5.1.4 Effect of cold work.....	36
2.5.1.5 Effect of processing parameters.....	37
2.5.1.6 Effect of resensitization and GBE study.....	37
2.5.2 Pitting corrosion behavior of LSM of stainless steels.....	38
2.5.2.1 Effect of heat treatment after LSM.....	39
2.5.2.2 Effect of processing parameters.....	39
2.5.2.3 Effect of shielding gas.....	40
CHAPTER 3: Experimental Details.....	46
3.1 Materials and isothermal aging.....	46

3.2 Laser surface melting.....	47
3.3 Corrosion test.....	49
3.3.1 Pitting corrosion test.....	50
3.3.2 DL-EPR test.....	51
3.4 Microstructural analysis.....	52
3.5 Hardness measurement.....	53
 CHAPTER 4: Results and Discussion: Effect of Heat Treatment on Intergranular and Pitting Corrosion Behavior of Stainless Steels.....	 55
4.1 Effect of isothermal aging on ASS, DSS and SDSS.....	55
4.1.1 Metallographic and microstructural analysis.....	55
4.1.2 Intergranular corrosion behavior.....	68
4.1.2.1 IGC of S34700 for aging time up to 720 h.....	68
4.1.2.2 IGC of various ASSs and DSSs aged for 40 h.....	73
4.1.3 Pitting corrosion behavior.....	80
4.1.3.1 Aged ASS S34700.....	82
4.1.3.2 Aged ASS FeCrMn.....	86
4.1.3.3 Aged DSS S31803.....	90
4.1.3.4 Aged DSS S32950.....	95
4.1.3.5 Aged SDSS S32760.....	99
 CHAPTER 5: Effect of Laser Surface Melting on Intergranular and Pitting Corrosion Behavior of Stainless Steels.....	 105
5.1 Effect of laser processing parameters on the pitting corrosion behavior of ASS FeCrMn and DSS S32950.....	105
5.1.1 Metallographic and microstructural analysis of FeCrMn.....	105
5.1.1.1 Single track LSM.....	105

5.1.1.2 LSM of full surface.....	110
5.1.1.3 Metallographic and microstructural analysis.....	112
5.1.2 Pitting corrosion behavior of FeCrMn.....	117
5.1.3 Metallographic and microstructural analysis of S32950.....	125
5.1.4 Pitting corrosion behavior of S32950.....	131
5.1.4.1 Aged S32950 after LSM.....	131
5.1.4.2 Aged S32950 for 200 h after LSM.....	136
5.2 IGC behavior of aged ASSs and DSSs after LSM.....	140
5.2.1 Metallographic and microstructural analysis.....	140
5.2.2 IGC behavior.....	151
5.2.2.1 Aged ASSs after LSM.....	157
5.2.2.2 Aged DSSs and SDSS after LSM.....	160
5.3 Effect of re-aging on the pitting corrosion behavior of ASS FeCrMn and DSS S32950.....	163
5.3.1 Effect of re-aging on the pitting corrosion behavior of ASS FeCrMn.....	163
5.3.2 Effect of re-aging on the pitting corrosion behavior of DSS S32950.....	167
CHAPTER 6: Conclusions.....	172
CHAPTER 7: Suggestions for further works.....	175
REFERENCES.....	176
Chapter 1.....	176
Chapter 2.....	179
Chapter 3.....	187
Chapter 4.....	188

Chapter 5.1.....	191
Chapter 5.2.....	192
Chapter 5.3.....	195
APPENDIX.....	196



LIST OF FIGURES

Figure 2.1 An optical micrograph showing a sensitized ASS.....	14
Figure 2.2 Isothermal precipitation diagram for DSS 2205, annealed at 1050 °C (Duplex grades 2304 and 2507 are shown for comparison)	16
Figure 2.3 Classification of laser remanufacturing technology	18
Figure 2.4 LSM processing diagram.....	19
Figure 2.5 Schematic illustration of flat free surface of LSM.....	21
Figure 2.6 A corrosion pit on the surface of a UNS S32304 stainless steel.....	27
Figure 2.7 Representative cyclic potentiodynamic polarization curves for UNS S30400 in 3.56 wt% NaCl solution at 25 ± 1 °C.	29
Figure 2.8 Hypothetical cathodic and anodic polarization plot for determining localized corrosion parameters.	30
Figure 2.9 A Typical IGC morphology of S30400 after DL-EPR test.....	32
Figure 2.10 Principle of DL-EPR technique and IGC sensitization criterion: (a) non-sensitized material and (b) sensitized material.	33
Figure 3.1 Focus point illustration.	48
Figure 3.2 Graphical illustration of calculating degree of overlapping.	49
Figure 3.3 Pitting corrosion test criteria for the stainless steels.	51
Figure 3.4 DL-EPR test criteria for the stainless steels.	52
Figure 4.1.1 SEM micrographs of S34700 aged at 600 °C for 720 h (etched by oxalic acid at 5V for 20 s).....	56
Figure 4.1.2 SEM micrographs of FeCrMn aged at 600 °C for (a) 4 h, (b) 50 h and (c) 200 h.....	57

Figure 4.1.3 SEM micrographs of S31803 aged at 800 °C for (a) solution-annealed, (b) 1 h, (c) 4 h, (d) 50 h, (e) 100 h and (f) 200 h (for (b) to (e), BSE image with EDX results in wt%), at a magnification of 500X.	60
Figure 4.1.4 BSE micrographs of S31803 aged at 800 °C for (a) solution-annealed, (b) 1 h, (c) 4 h, (d) 50 h, (e) 100 h and (f) 200 h, at a magnification of 1000X.	61
Figure 4.1.5 SEM micrographs of S32950 for (a) annealed (b) 4 h, (c) 50 h and (d) 200 h aged at 800°C.....	62
Figure 4.1.6 XRD spectra of various aging time of S32950.....	63
Figure 4.1.7 SEM micrographs of S32760 aged at 800°C for (a) solution-annealed, (b) 1 h, (c) 4 h, (d) 50 h, (e) 100 h and (f) 200 h (For (b) to (e), BSE image with EDX results in wt%), at a magnification of 500X.	67
Figure 4.1.8 BSE micrographs of S32760 aged at 800 °C for (a) solution-annealed, (b) 1 h, (c) 4 h, (d) 50 h, (e) 100 h and (f) 200 h, at a magnification of 1000X.	68
Figure 4.1.9 DL-EPR curves for aged S34700 up to 720 h in 0.5 M H ₂ SO ₄ + 0.01 M KSCN solution at 25 °C.....	69
Figure 4.1.10 DOS value plot against aging time of S34700.	70
Figure 4.1.11 Corrosion morphologies of S34700 after DL-EPR test which aged at (a) 40 h, (b) 200 h, (c) 333 h, (d) 455 h, (e) 575 h and (f) 720 h.....	71
Figure 4.1.12 (a) Corrosion morphology of aged S34700 after DL-EPR test and (b) EDX spectrum of Nb-rich phase.....	72
Figure 4.1.13 Schematic illustration of newly proposed IGC mechanism developed by Cr-depletion due to segregation of the un-reacted Cr atoms in the grain boundary area	73
Figure 4.1.14 DL-EPR curves for (a) aged S30400, S31603, S32100, S34700 (aged for 720 h) and FeCrMn before LSM in 0.5 M H ₂ SO ₄ + 0.01 M KSCN solution at 25	

°C and (b) aged S31803, S32950 and S32760 before LSM in 2 M H ₂ SO ₄ + 0.01 M KSCN + 0.5M NaCl solution at 25 °C.....	75
Figure 4.1.15 Corrosion morphologies of aged ASSs after DL-EPR test (a) S30400, (b) S31603, (c) S32100, (d) S34700, and (e) FeCrMn.....	78
Figure 4.1.16 Corrosion morphologies of aged DSSs and SDSS after DL-EPR test (a) S31803, (b) S32950 and (c) S32760.....	80
Figure 4.1.17 Cyclic polarization curves of (a) S34700, (b) FeCrMn, (c) S31803 (d) S32950 and (d) S32760 aged at various time up to 200 h.....	82
Figure 4.1.18 Corrosion parameters for aged S34700 up to 200 h (a) E _{corr} , (b) I _{corr} , (c) I _{pass} (d) E _{pit} and (e) E _{prot}	84
Figure 4.1.19 Corrosion morphology of aged S34700 for (a) annealed (b) 4 h, (c) 50 h and (d) 200 h after cyclic polarization test.....	86
Figure 4.1.20 Corrosion parameters for aged FeCrMn up to 200 h (a) E _{corr} , (b) I _{corr} , (c) I _{pass} (d) E _{pit} and (e) E _{prot}	88
Figure 4.1.21 Corrosion morphology of Aged FeCrMn for (a) annealed (b) 4h, (c) 50h and (d) 200 h after cyclic polarization test.....	90
Figure 4.1.22 Corrosion parameters for aged S31803 aged up to 200h (a) E _{corr} , (b) I _{corr} , (c) I _{pass} (d) E _{pit} and (e) E _{prot}	93
Figure 4.1.23 Corrosion morphology of aged S31803 for (a) annealed (b) 4 h, (c) 50 h and (d) 200 h after cyclic polarization test at a magnification of 200X.	94
Figure 4.1.24 Corrosion morphology of aged S31803 for (a) annealed (b) 4 h, (c) 50 h and (d) 200 h after cyclic polarization test at a magnification of 1000X.	95
Figure 4.1.25 Corrosion parameters for aged S32950 aged up to 200 h (a) E _{corr} , (b) I _{corr} , (c) I _{pass} (d) E _{pit} and (e) E _{prot}	98
Figure 4.1.26 Corrosion morphology of aged S32950 for (a) 4 h, (b) 50 h and (c) 200	

h after cyclic polarization test.	98
Figure 4.1.27 Corrosion parameters for S32760 aged up to 200 h (a) E_{corr} , (b) I_{corr} , (c) I_{pass} , (d) E_{pit} and (e) E_{prot}	102
Figure 4.1.28 Corrosion morphology of aged S32760 for (a) annealed (b) 4 h, (c) 50 h and (d) 200 h after cyclic polarization test at a magnification of 200X.	103
Figure 4.1.29 Corrosion morphology of aged S32760 for (a) annealed (b) 4h, (c) 50h and (d) 200h after cyclic polarization test at a magnification of 1000X.	104
Figure 5.1.1 Cross-sectional views of various LSM specimens.	107
Figure 5.1.2 Data plots of various sets of laser processing parameters.	109
Figure 5.1.3 Surface appearances and cross-sectional views of the specimens fabricated at various laser processing conditions after LSM.	112
Figure 5.1.4 EDX spectrum of as-received FeCrMn stainless steel.	114
Figure 5.1.5 A typical transverse cross-sectional view of LSM specimen (L20).	114
Figure 5.1.6 XRD spectrum of LSM specimen (L20).	115
Figure 5.1.7 Microstructures of melt zone of laser-melted FeCrMn for the processing parameter (a) L17 (b) L20, (c) L25 and (d) L28.	116
Figure 5.1.8 EDX spectra of (a) melt pool and (b) substrate for L17.	116
Figure 5.1.9 Hardness profile along the depth of the cross-section of melt pool (a) L17 and (b) L28.	117
Figure 5.1.10 Cyclic polarization curves of laser-melted FeCrMn with various laser processing parameters.	119
Figure 5.1.11 Corrosion parameters of FeCrMn at various scanning speeds.	123
Figure 5.1.12 Corrosion parameters of FeCrMn at various beam diameters.	124
Figure 5.1.13 Corrosion morphology of (a) as-received and (b) L20 after cyclic polarization test.	125

Figure 5.1.14 SEM micrographs of aged S32950 (for 200 h) laser-melted with processing condition L1 (a) cross-sectional view; and (b) microstructure of melt zone.	126
Figure 5.1.15 SEM micrographs of aged S32950 (for 200h) laser-melted with processing condition L2 (a) cross-sectional view; and (b) microstructure of melt zone.	127
Figure 5.1.16 SEM micrographs of aged S32950 (for 200 h) laser-melted with processing condition L3 (a) cross-sectional view; and (b) microstructure of melt zone.	127
Figure 5.1.17 XRD spectra of various aging time after LSM of parameter L1.....	128
Figure 5.1.18 XRD spectra aged at 200 h after LSM with various laser parameters.	129
Figure 5.1.19 Harness profiles of S32950 aged for 200 h after LSM with L1, L2 and L3.	130
Figure 5.1.20 Polarization curves of aged S32950 laser-melted with L1.....	132
Figure 5.1.21 Polarization curves of aged S32950 laser-melted with L2.	133
Figure 5.1.22 Polarization curves of aged S32950 laser-melted with L3.....	134
Figure 5.1.23 Corrosion parameters for aged S32950 after LSM (a) E_{corr} (b) E_{pit} and (c) E_{prot}	135
Figure 5.1.24 Corrosion parameters for aged S32950 after LSM (a) I_{corr} and (b) I_{pass}	136
Figure 5.1.25 Polarization curves of laser-melted, aged and annealed S32950.....	137
Figure 5.1.26 Corrosion morphology of (a) aged S32950 for 200 h, (b) aged S32950 laser-melted with L1 (c) aged S32950 laser-melted with L2 (d) aged S32950 laser-melted with L3.	139

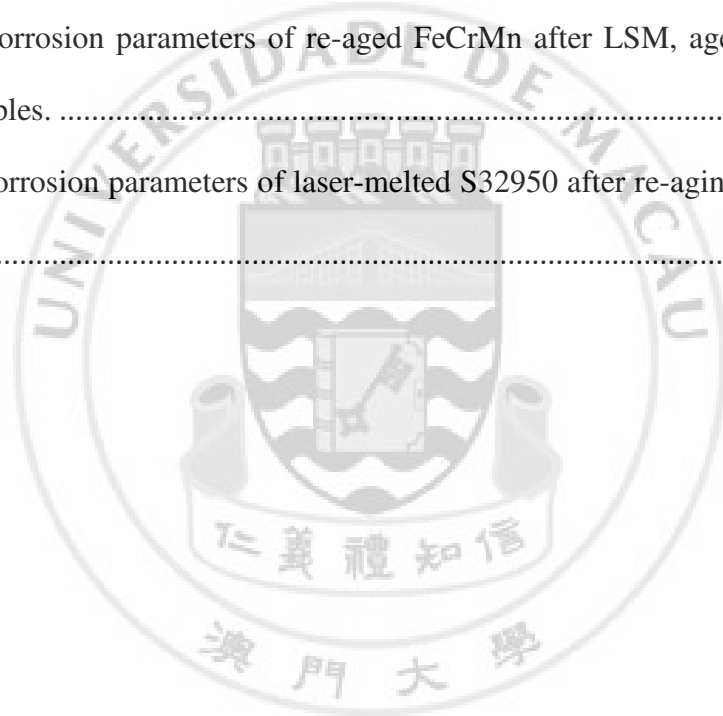
Figure 5.2.1 SEM micrographs of LM-30400-S (a) cross-sectional view (OM) and (b) microstructure of melt pool (SE image with EDX results).....	140
Figure 5.2.2 SEM micrographs of LM-31603-S (a) cross-sectional view (OM) and (b) microstructure of melt pool (SE image with EDX results).....	141
Figure 5.2.3 SEM micrographs of LM-32100-S (a) cross-sectional view (OM) and (b) microstructure of melt pool (SE image with EDX results).....	141
Figure 5.2.4 SEM micrographs of LM-34700-S (a) cross-sectional view (OM) and (b) microstructure of melt pool (SE image with EDX results).....	142
Figure 5.2.5 SEM micrographs of LM-FeCrMn-S (a) cross-sectional view (OM) and (b) microstructure of melt pool (SE image with EDX results in wt%, IB = interdendritic boundary).....	142
Figure 5.2.6 SEM micrographs of LM-S31803 (a) cross-sectional view (OM), (b) microstructure of melt pool (SE image with EDX results in wt%), and (c) microstructure of sensitized zone (BSE image with EDX results in wt%).....	143
Figure 5.2.7 SEM micrographs of LM-S32950-S (a) cross-sectional view (OM), (b) microstructure of melt pool (BSE image with EDX results in wt%), and (c) microstructure of aged substrate (BSE image with EDX results in wt%).	144
Figure 5.2.8 SEM micrographs of LM-S32760-S (a) cross-sectional view (OM), (b) microstructure of melt pool (BSE image with EDX results in wt%), and (c) microstructure of aged substrate (BSE image with EDX results in wt%).	145
Figure 5.2.9 Hardness of various stainless steels in annealed, aged and laser-melted conditions.....	149
Figure 5.2.10 DL-EPR curves for aged (a) S30400, (b) S31603, (c) S32100, (d) S34700, and (e) FeCrMn before and after LSM in 0.5 M H ₂ SO ₄ + 0.01 M KSCN	

solution at 25 °C.	154
Figure 5.2 11 DL-EPR curves for aged (a) S31803, (b) S32950 and (c) S32760 before and after LSM in 2 M H ₂ SO ₄ + 0.01 M KSCN + 0.5M NaCl solution at 25 °C.	155
Figure 5.2 12 Corrosion morphologies of aged ASSs after DL-EPR test (a) S30400, (b) S31603, (c) S32100, (d) S34700, and (e) FeCrMn (i) before LSM and (ii) after LSM.	156
Figure 5.2.13 Corrosion morphologies of aged DSSs and SDSS after DL-EPR test (a) S31803, (b) S32950 and (c) S32760 (i) before LSM and (ii) after LSM.....	157
Figure 5.3.1 Polarization curves of laser-melted FeCrMn after re-aging for 50 h and annealed specimens.....	164
Figure 5.3.2 Polarization curves of (a) L20 and re-aged L20, (b) L28 and re-aged L28.	166
Figure 5.3.3 Corrosion morphology of re-aged L20 after polarization test.....	167
Figure 5.3.4 Polarization curves of laser-melted S32950 after re-aging for 200h, annealed and aged specimens.	168
Figure 5.3.5 Polarization curves of (a) L1 and re-aged L1, (b) L2 and re-aged L2, and (c) L3 and re-aged L3.	170
Figure 5.3.6 Corrosion morphology of (a) aged S32950 for 200h, (b) re-aged S32950 laser-melted with L1 (c) re-aged S32950 laser-melted with L2 and (d) re-aged S32950 laser-melted with L3.	171

LIST OF TABLES

Table 2.1 A summary of research on laser surface melting of stainless steels for mitigating IGC.	43
Table 2.2 A summary of research on LSM of stainless steels for improving pitting corrosion resistance.....	45
Table 3.1 Compositions of various stainless steels in wt%.	47
Table 3.2 Processing parameters for LSM of 7MoPlus.	47
Table 3.3 Processing parameters for LSM of FeCrMn.	49
Table 4.1.1 DOS of S34700 at various aging time after DL-EPR test.....	69
Table 4.1.2 DOS of various stainless steels after DL-EPR test.	74
Table 4.1.3 Corrosion parameters of S34700 from cyclic polarization test.....	85
Table 4.1.4 Corrosion parameters of FeCrMn from cyclic polarization test.	89
Table 4.1.5 Corrosion parameters of S31803 from cyclic polarization test.....	93
Table 4.1.6 Corrosion parameters of S32950 from cyclic polarization test.....	96
Table 4.1.7 Corrosion parameters of S32760 from cyclic polarization test.....	102
Table 5.1.1 Various single-track laser processing parameters for FeCrMn.	106
Table 5.1.2 Laser processing parameters and degree of overlapping for various specimens.....	111
Table 5.1.3 Chemical compositions of ASSs S30400 and FeCrMn (the content of the elements is in wt-%).....	114
Table 5.1. 4 Chemical compositions of L17 (a) melt pool and (b) substrate.	116
Table 5.1.5 Corrosion parameters of laser-melted FeCrMn at different laser processing parameters.	120

Table 5.1.6 Processing parameters for LSM.	126
Table 5.1.7 Corrosion parameters of laser-melted S32760 (L1).	133
Table 5.1.8 Corrosion parameters of laser-melted S32760 (L2).	133
Table 5.1.9 Corrosion parameters of laser-melted S32760 (L3).	134
Table 5.1.10 Corrosion parameters of laser-melted, aged and annealed S32950.	137
Table 5.2.1 Cr_{eq}/Ni_{eq} ratio, phase present and volume fraction of ferrite (C_{δ}) in aged stainless steels before and after LSM.	150
Table 5.2.2 DOS of various stainless steels after DL-EPR test.	152
Table 5.3.1 Corrosion parameters of re-aged FeCrMn after LSM, aged for 50 h and annealed samples.	165
Table 5.3.2 Corrosion parameters of laser-melted S32950 after re-aging, annealed and aged S32950.	168



LIST of Abbreviations

ASS	Austenitic Stainless Steel
ASTM	America Society of Testing and Materials
DOS	Degree of Sensitization
DSS	Duplex Stainless Steel
E_{corr}	Corrosion Potential
EDX	Energy Dispersive Spectroscopy
E_{pit}	Pitting Potential
E_{prot}	Protection Potential
FSS	Ferrite Stainless Steel
I_{corr}	Corrosion Current
IGC	Intergranular Corrosion
I_{pass}	Passivation Current
ISO	International Organization for Standardization
LC	Laser Cladding
LSA	Laser Surface Alloying
LSM	Laser Surface Melting
OCP	Open Circuit Potential
OM	Optical Microscope
PC	Pitting Corrosion
SDSS	Super Duplex Stainless Steel
SEM	Scanning Electron Microscope
XRD	X-Ray Diffractometry

LIST OF PUBLICATIONS

Book Chapter

1. **W.K. Chan**, C.T. Kwok, K.H. Lo, Chapter 3. Laser surface melting of stainless steels for mitigating intergranular corrosion, in 'Laser Surface Modification of Alloys for Erosion and Corrosion Resistance', C.T. Kwok (Editor), Woodhead Publishing, ISBN 13: 9780857090157 ISBN 10: 0857090151 (to be published in 2012)

Journal Paper

1. C.T. Kwok, K.H. Lo, **W.K. Chan**, F.T. Cheng, H.C. Man, Effect of laser surface melting on intergranular corrosion behaviour of aged austenitic and duplex stainless steels, Corrosion Science, 53 (2011) pp.1581-1591. (SCI, Impact factor: 3.261)

Conference Papers

1. **W.K. Chan**, C.T. Kwok, K.H. Lo, 'Effect of Laser Surface Melting on Corrosion Behavior of Aged Duplex Stainless Steel', Proceedings of the 29th International Congress on Applications of Lasers & Electro-Optics 2010 (ICALEO '10), Anaheim, CA, USA, 27-30 Sept. (2010). (EI)
2. C.T. Kwok, P.K. Wong, **W. K. Chan**, F.T. Cheng, H.C. Man, 'Laser Surface Alloying of Mn-Ni-Al Bronze for Cavitation Erosion Resistance', Proceedings of

the 29th International Congress on Applications of Lasers & Electro-Optics 2010 (ICALEO '10), Anaheim, CA, USA, 27-30 Sept. (2010). (EI)

3. **W.K. Chan**, C.T. Kwok, K.H. Lo, Z. Cheng, 'Desensitization of Austenitic and Duplex Stainless Steels by Laser Surface Melting', Proceedings of the 3rd Pacific International Conference on Application of Lasers and Optics (PICALO 2010), March 23 – 25, Wuhan, China. (EI)
4. P.K. Wong, **W.K. Chan**, C.T. Kwok, K.H. Lo, 'Applications of laser remanufacturing for wear and corrosion resistance', Proceedings of 6th International Symposium on Environmentally Conscious Design and Inverse Manufacturing (EcoDesign 2009), December 7-9, 2009, Sapporo, Japan, pp.303-307.
5. **W.K. Chan**, C.T. Kwok, K.H. Lo, S.F. Wong, 'The Critical Part of PEMFC – Super Duplex Stainless Steel Bipolar Plates' 6th International Symposium on Environmentally Conscious Design and Inverse Manufacturing (EcoDesign 2009), December 7-9, 2009, Sapporo, Japan, pp.1185-1190

ACKNOWLEDGMENTS

Firstly, I would like to express my sincere appreciation to my supervisor Prof. Kwok Chi Tat and co-supervisor Dr. Lo Kin Ho for their kind supports and guidance on my research work during graduate study. Besides conducting research work in UM, I have chance to attend two international conferences during my master study, I would like to acknowledge Prof. Kwok once again for giving me such good opportunities to open my mind and share his experience with me.

Also, I would like to thank Ms. Wong Po Kee and Mr. Zhang Bo Kai for their help and technical supports in the Corrosion and Metallography Laboratory, Laser Laboratory and SEM Laboratory; in addition, I wish to acknowledge the supports from the infrastructure of the University of Macau, the academic and administrative staff in the Department of Electromechanical Engineering, and also the financial support from Science and Technology Development Fund of Macau (FDCT).

Finally, I would like to express my sincere thanks to my beloved friends and family for their support and encouragement. Last but not least, I would like to thank God for being the guidance of my life.